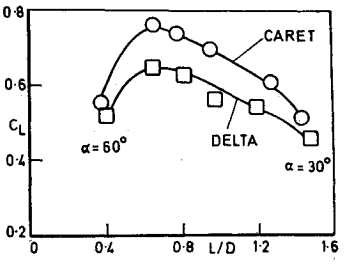

Fig. 3 Lift coefficients.

The experimental data has been tabulated by Coleman.[5]

The measurements of normal force coefficient, C_N, for the flat delta and caret wing models are compared with each other and with some theoretical predictions in Fig. 2. The caret wing develops significantly higher values of C_N than does the flat delta. Near the caret design incidence ($\alpha = 34°$) the experimental values agree well with the two-dimensional (wedge) prediction whereas, at the same incidence, C_N for the delta wing corresponds more closely to the cone value. Similar comments were found to apply to the measured shock wave angles. Simple Newtonian theory ($C_p = 2 \sin^2\alpha$) also gives a good estimate of C_N for the flat delta over the incidence range considered, but tends towards underestimation at low α and overestimation at high α. The agreement of Squire's prediction[6] for the caret wing is striking, but for the flat delta his method is less successful.

The lift coefficients (C_L) developed by the two models are compared in Fig. 3; the superiority of the caret wing over the entire incidence range is clear. Both shapes develop maximum lift around 50° incidence, corresponding to $L/D \simeq 0.7$.

4. Conclusions

Tests have been conducted at a Mach number of 9 to compare the performance of a flat-bottomed delta and a caret wing model at high angles of incidence appropriate to lifting re-entry conditions. The distinct advantage of the caret wing over the incidence range considered has been clearly shown. Comparisons between the data and a few prediction methods for the normal force coefficient have been made and particularly good agreement has been found between the data and Squire's theoretical curve for the caret wing.

References

[1] Opatowski, T. P. S., "An Experimental Study of the Flow around and the Forces Developed by Hypersonic Lifting Vehicles," Ph.D. thesis, 1969, University of London, London, England.

[2] Rao, D. M., "Hypersonic Aerodynamic Characteristics of Flat Delta and Caret Wings at High Incidence Angles," *Journal of Spacecraft and Rockets*, Vol. 7, No. 12, Dec. 1970, pp. 1475–1476.

[3] Carr, C. J., "Force Measurements on Caret and Delta Wings over the Incidence Range $27° < \alpha < 55°$ at $M = 12.2$," Aero Rept. 71-22, Oct. 1971, Imperial College of Science and Technology, London, England.

[4] Needham, D. A., Elfstrom, G. M., and Stollery, J. L., "Design and Operation of the Imperial College No. 2 Hypersonic Gun Tunnel," Aero Rept. 70-04, 1970, Imperial College of Science and Technology, London, England.

[5] Coleman, G. T., "Force Measurements on Caret and Delta Wings at High Incidence," Aero Rept. 72-16, July 1972, Imperial College of Science and Technology, London, England.

[6] Squire, L. C., "Calculations of the Pressure Distribution on lifting Conical Wings with Applications to the Off-design Behaviour of Caret Wings," AGARD CP 30, 1968.

Viscous Damping Characteristics of Dacron Parachute Suspension-Line Cord

LAMONT R. POOLE*
NASA Langley Research Center, Hampton, Va.

Introduction

A KEY element in the analytical study of parachute inflation dynamics is the calculation of loads exerted on the towing vehicle by the inflating parachute. Recent analyses[1,2] have shown that suspension-line elasticity and viscous damping can have an important effect on the magnitude of the opening load exerted on the vehicle.

This Note presents results obtained from a test program conducted to determine the force-strain characteristics of Type 52, 220-denier, 880-lb minimum tensile strength dacron suspension-line cord under quasi-static loading conditions and at strain rates ranging up to 210%/sec. Average force-strain curves were obtained, and viscous damping coefficient curves approximating the change in response attributed to dynamic loading conditions were calculated. The calculated damping coefficient was observed to be a nonlinear function of both strain and strain rate. Rupture loads measured during the test program were observed to decrease with increasing strain rate.

Test System Description

The basic Type 52 dacron cord was first cut into sections, which were then heat sterilized according to Viking specifications. After sterilization, the sections were formed into test samples having Chinese-finger end loops and a pin-to-pin length of 15 in.

Quasi-static tensile tests were performed on an Instron tensile-testing machine. Dynamic tensile tests were performed by using a hydraulically-driven ram mechanism which is sketched in Fig. 1. Samples were attached to pin-type fittings on the ram head and on a rigid base by using the Chinese-finger end loops. Ram-head displacement was measured by using a steel-cable-driven potentiometer: dynamic effects on the steel cable were considered to be negligible. Force

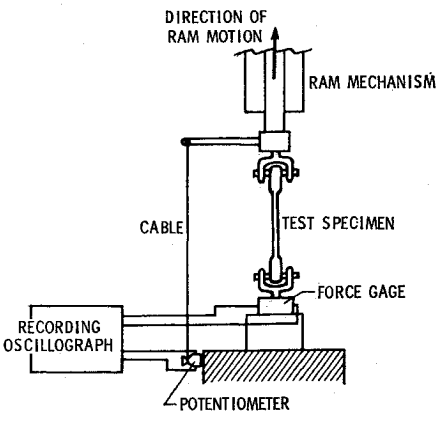

Fig. 1 Sketch of test system configuration.

Presented as Paper 73-446 at the AIAA 4th Aerodynamic Deceleration Systems Conference, Palm Springs, Calif., May 21–23, 1973; submitted May 11, 1973; revision received June 22, 1973.

Index categories: Materials, Properties of; Entry Deceleration Systems and Flight Mechanics (e.g., Parachutes).

* Aerospace Technologist, Space Applications and Technology Division.

was measured by using a dynamically calibrated resistance-type force gage which was attached to the rigid base. A recording oscillograph was used for simultaneous recording of displacement and force measurements.

Test Results

A series of tensile tests was performed under quasi-static loading conditions and at each of several strain rates ranging up to 210%/sec. Strain rates were calculated as the ratio of the essentially constant ram-head velocity to the 15-in. pin-to-pin specimen length. All tests were initiated with the test samples slack in order to allow the machine head to attain a constant speed before load was applied. Then the test samples were strained continuously to the point of rupture.

Force-strain curves were obtained for each of the individual tensile tests. The individual curves were grouped according to strain rate, and then the groups were screened so that those groups which exhibited excessive scatter between the individual curves in the group could be deleted from further analysis. Average force-strain curves were then calculated for the remaining groups, which included the quasi-static tests and tests conducted at the 50%, 140%, and 210%/sec strain-rate levels. These average curves are shown in Fig. 2.

The change in response attributed to dynamic loading conditions was determined by mechanically integrating each of the four average force-strain curves over 0.04 strain intervals, and then, for each interval, subtracting the area under the quasi-static curve from the area under each of the other curves. The viscous damping coefficient was calculated by dividing the average of each of the area differences for each interval by the corresponding strain rate. Curves of the computed damping coefficient for the strain rates of 50%, 140%, and 210%/sec are shown in Fig. 3, with actual computed values plotted at the midpoints of the strain intervals over which the area differences were averaged. Uncertainty in the computed curves is an inverse function of strain rate and is estimated to range from about ±5% for the 210%/sec curve to about ±20% for the 50%/sec curve. The curves in Fig. 3 indicate that the damping coefficient is a nonlinear function of both strain and strain rate.

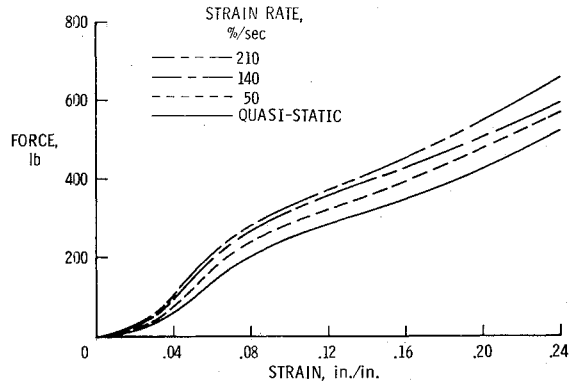

Fig. 2 Average force-strain curves.

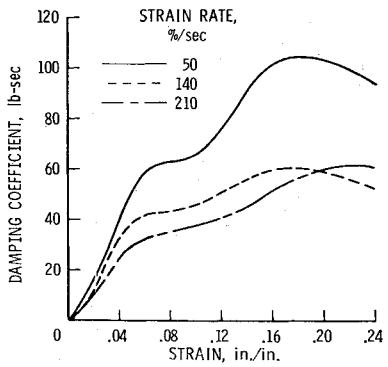

Fig. 3 Computed damping coefficient curves.

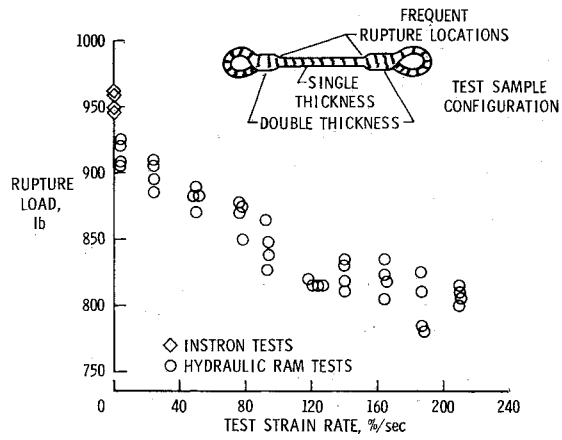

Fig. 4 Measured rupture loads as a function of test strain rate.

Another interesting feature of the test data is the decrease in recorded rupture loads with increasing strain rate, as shown in Fig. 4. Included in this figure are the rupture loads recorded for all tests which were performed in the test program. Several possible reasons for this decrease in rupture load can be noted. All sample ruptures were observed to occur in the single-thickness region of the samples, but near the junctures of this region and the double-thickness region of the Chinese-finger end loops (see insert, Fig. 4). Location of the ruptures possibly indicates some type of stress concentration caused by combined loading at the interior end of the Chinese-finger loops. Also, although no exact measurements were made, the temperature of the samples was observed to increase markedly with increasing test strain rate. At the higher strain rates, fractured dacron strands were observed to fuse together after rupture. This observation possibly suggests some thermodynamic cause of the decrease in rupture loads.

Conclusions

A test program has been conducted to investigate the viscous damping characteristics of Type 52, 220-denier dacron suspension-line cord. Based on the results of this program, the following conclusions can be stated: 1) The viscous damping coefficient is a nonlinear function of both strain and strain rate. 2) The rupture loads measured in the text program decreased with increasing strain rate, possibly due to stress concentrations induced by the test-sample configuration or to internal thermodynamics.

References

[1] Preisser, J. S. and Greene, G. C., "Effect of Suspension Line Elasticity on Parachute Loads," *Journal of Spacecraft and Rockets*, Vol. 7, No. 10, Oct. 1970, pp. 1278–1280.

[2] Poole, L. R., "Effect of Suspension-Line Viscous Damping on Parachute Opening Load Amplification," *Journal of Spacecraft and Rockets*, Vol. 10, No. 1, Jan. 1973, pp. 92–93.